DOI: 10.13009/EUCASS2025-415
11TH EUROPEAN CONFERENCE FOR AERONAUTICS AND SPACE SCIENCES (EUCASS)

ROTOR DYNAMICS DESIGN CONCERNS OF A SINGLE-SHAFT TURBOPUMP FOR DEEP THROTTLING ENGINES

Wonil KWAK*†, Kangmin LEE, Myeong-Seok GO, Jungwan KIM, Byung Ju LEE,
Jung Shin PARK, Joo Hoon PARK, Jinsoo LEE, Wonsuk LEE

* † *Engine R&D Team, Space Launch R&D Center, Hanwha Aerospace, Daejoen, Republic of Korea Address*

wonil.kwak@hanwha.com

Abstract

This study presents a design approach to address critical speed transitions and rotordynamic instabilities in turbopumps for deep throttling liquid rocket engines used in reusable launch vehicles. Variations in rotational speed, axial load, and support stiffness during throttling operations can significantly affect system stability. The critical speed locations and stability margins are quantitatively evaluated, with the goal of identifying safe operating ranges that avoid instability zones. To this end, a dynamic analysis framework for the bearing-seal support system is developed, incorporating thermal deformation effects on bearing contact conditions. Parametric studies under realistic operating conditions are conducted to assess the system's dynamic behavior. Based on these findings, an integrated rotor-support design methodology is proposed to ensure stable operation across the entire throttling range, providing a key technological foundation for enhancing the reliability and operational life of reusable liquid rocket engines.

1. Introduction

Deep throttling is a control technique in liquid rocket engines that allows operation at thrust levels significantly lower than the nominal rating—often below 20%. This capability is regarded as a key enabling technology for reusable launch vehicles, as it facilitates precise orbital insertion and controlled landing maneuvers. Thrust adjustment is typically achieved by regulating the flow rate or inlet pressure of fuel and oxidizer, which consequently alters the combustion chamber pressure and gas temperature. These changes significantly affect the boundary conditions at the turbine and pump stages, leading to substantial variations in turbopump rotational speed and axial thrust.

Conventional turbopumps are designed to operate stably within a narrow range around their rated conditions. However, these assumptions may no longer hold under deep throttling conditions. The rotor system is subjected to wide-ranging speed changes and varying axial loads, which can push the system across its critical speeds. In particular, abrupt shifts in rotational speed may result in resonance near critical frequencies, and any discrepancy between the predicted and actual behavior of bearing–seal support systems may induce vibration instability and reduce service life. According to the *European Staged Combustion Engine Roadmap*, high-pressure fuel and oxidizer turbopumps are often required to operate between the first and second critical speeds, making the assurance of rotordynamic stability a core requirement in design [1].

The theoretical foundation for analyzing these challenges is rooted in the work of Childs [2] who established a comprehensive framework for modeling fluid-induced forces, dynamic stiffness, damping, and stability thresholds in rotor–bearing–seal systems. His analysis of fluid-structure interactions in high-speed rotating systems has served as a basis for numerous follow-up studies. However, despite the extensive theoretical groundwork, dedicated research specifically focused on turbopump rotor systems remains relatively scarce.

In recent years, several relevant studies have been published. For instance, Zhang et al. [3] demonstrated that variations in dynamic stiffness of aerospace engine bearings within certain frequency ranges can lead to decreased system stability, with thermal and centrifugal effects identified as major contributing factors. In a separate investigation, Lei et al. [6] examined how thermal deformation and unsteady flow within honeycomb seal structures influence rotor–seal interactions, using both experimental data and numerical models. Additionally, recent research on nonlinear fluid

Copyright © 2025 by First Author. Posted online by the EUCASS association with permission.

DOI: 10.13009/EUCASS2025-415

support elements, such as swirl brakes and gas film seals, has introduced coupled CFD–system-level simulations to evaluate damping characteristics near critical speeds. These efforts share a technical alignment with the present study, which seeks to quantify rotordynamic behavior under throttling conditions.
Nevertheless, most existing studies remain limited to static or simplified boundary conditions, or they are constrained to component-level analyses. There is a clear lack of comprehensive system-level investigations that address how dynamic characteristics evolve when multiple operational variables—such as rotational speed, axial thrust, and thermal deformation—change simultaneously. Furthermore, the dynamic response of bearing–seal systems under such conditions and its impact on the system's overall stability margin has yet to be thoroughly quantified. There is also a gap in studies that integrate the effects of critical speed transitions, damping variation, and design-to-performance mismatch into a holistic design methodology.
To address these gaps, this study aims to answer the following key research questions:

1. How can the timing and characteristics of critical speed crossings under deep throttling conditions be quantitatively identified?
2. In what ways do variations in rotational speed, axial thrust, and thermally induced deformation influence the dynamic stiffness and damping of bearing–seal support systems?
3. Can a fully coupled analytical framework be developed to ensure dynamic stability across the entire throttling envelope?

This study extends Childs' foundational theory by incorporating thermal deformation effects into the modeling of bearing contact conditions and by developing a bearing–seal dynamic analysis approach applicable under realistic operating scenarios. A parametric study is conducted to evaluate system behavior, with the ultimate goal of proposing an integrated rotor–support design methodology that secures stability margins and avoids critical speed crossings throughout the deep throttling range. This framework contributes to advancing the durability and reliability of next-generation reusable rocket engines.

2. Background and Literature Review

2.1 Deep Throttling Effects on Rotordynamic Stability: Theoretical Background

Deep throttling in liquid rocket engines refers to operating the engine at thrust levels significantly lower than rated conditions—often below 20%—to enable precise orbital insertion and controlled landing maneuvers, particularly in reusable launch vehicles. Thrust reduction is typically achieved by regulating propellant flow and pressure, which subsequently changes turbine and pump inlet conditions. These variations result in large fluctuations in turbopump rotational speed and axial thrust, which significantly affect the rotor system's dynamic behavior.
Conventional turbopump designs are optimized for steady-state performance at rated operating conditions. However, under deep throttling, the rotor can approach or pass through critical speeds, where dynamic instabilities are likely to occur. These phenomena manifest as increased vibration amplitudes, synchronous whirl, and degraded bearing and seal performance due to mismatches between predicted and actual support behavior. The *European Staged Combustion Engine Roadmap* emphasizes that high-pressure turbopumps in modern engines are often expected to operate between the first and second critical speeds, requiring high-fidelity dynamic models to ensure stability across such operating envelopes [1].
Figure 1 shows the basic rotordynamic model and advanced turbopump rotordynamic model.
The theoretical framework for modeling rotor–bearing–seal systems under these conditions was established by Childs, who formulated a linearized dynamic model incorporating stiffness and damping coefficients, including destabilizing cross-coupled terms caused by hydrodynamic forces. The fluid-induced forces acting on the rotor are expressed as:

$$\begin{bmatrix} F_x \\ F_y \end{bmatrix} = \begin{bmatrix} K_{xx} & K_{xy} \\ K_{yx} & K_{yy} \end{bmatrix} \cdot \begin{bmatrix} x \\ y \end{bmatrix} + \begin{bmatrix} C_{xx} & C_{xy} \\ C_{yx} & C_{yy} \end{bmatrix} \cdot \begin{bmatrix} \dot{x} \\ \dot{y} \end{bmatrix} \quad (1)$$

where:

- F_x, F_y are the dynamic forces,
- x, y are the rotor displacements,
- ẋ, ẏ are velocity components,
- K_{ij} and C_{ij} represent stiffness and damping coefficients, with Kxy and Kyx responsible for forward-whirl instabilities.

DOI: 10.13009/EUCASS2025-415

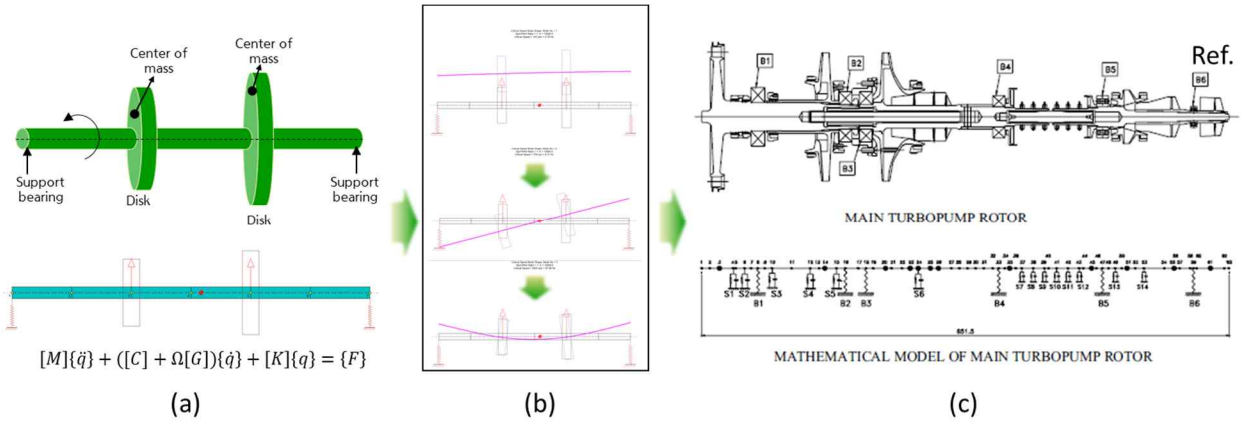

Figure 1: (a) Basic rotordynamic model (b) Critical mode shape results, (c) Turbopump rotordynamic model [4]

These forces are incorporated into the complete equation of motion:

$$M \cdot \ddot{q}(t) + C \cdot \dot{q}(t) + K \cdot q(t) = F_{fluid}(t) \quad (2)$$

where:

- $q(t) = [x(t), y(t)]^T$ is the displacement vector,
- M is the mass matrix,
- C and K are damping and stiffness matrices,
- $F_{fluid}(t)$ is the applied fluid force vector.

In deep throttling regimes, reduced damping, shifting axial loads, and thermally induced deformations significantly alter the effective support characteristics, magnifying the destabilizing effect of cross-coupled stiffness terms. Thus, accurate modeling of K_{xy} and K_{yx} —along with their dependence on temperature and preload variations—is essential to predicting instability thresholds and designing robust rotor-support systems.
This combined theoretical framework is employed in the present study as a foundation for extending rotordynamic analysis into the deep throttling operating domain of reusable rocket turbopumps.

2.2 Recent Developments in Bearing and Seal Dynamics

Recent research has focused on improving the accuracy of stiffness predictions in bearing systems by incorporating nonlinearity, speed dependency, and thermal effects. Zhang et al. [3] introduced a model that includes inner ring elastic deformation to quantify the influence of interference fits, rotational speed, and radial load on bearing stiffness. Gunduz and Singh [4] developed a detailed stiffness matrix formulation for double-row angular contact ball bearings, revealing the sensitivity of stiffness coefficients to geometric and kinematic variables.
To address deformation effects under combined loading, Lei et al. [6] proposed an integrated stiffness model that accounts for elastic, centrifugal, and thermal deformations, offering improved predictive capability for both axial and radial stiffnesses. On the geometric optimization side, Deng et al. [7] employed a nonlinear dynamic model to investigate how variations in ball count and groove curvature radii affect bearing stiffness. Their work integrates the effects of cage dynamics, lubrication, and thermal behavior into a comprehensive framework. Xu et al. [8] further expanded this by formulating a five-dimensional stiffness matrix for duplex angular contact bearings under different misalignment configurations, a scenario highly relevant for high-speed rotating equipment with assembly tolerances and preload variation.
While these studies have advanced the modeling of bearing and seal dynamics under various operating conditions, most remain limited to simplified or static boundary assumptions. There is a distinct lack of system-level investigations that evaluate how dynamic characteristics evolve when multiple operational variables—such as rotational speed, axial thrust, and thermally induced deformation—change simultaneously. In particular, the interaction between critical speed crossings, damping variation, and preload shifts remains underexplored. Furthermore, few studies have addressed how these coupled effects influence overall system stability margins or how they can be incorporated into robust rotor-support design strategies.

DOI: 10.13009/EUCASS2025-415

To address this gap, the present study proposes a fully integrated rotordynamic analysis framework tailored for deep throttling operations. By extending Childs' theoretical foundation to include thermal deformation effects and parametric sensitivity under real-world conditions, this work aims to identify safe operating regions, evaluate stability boundaries, and develop design methods that secure rotordynamic integrity across the full throttling envelope. This contribution is essential for advancing the reliability and service life of next-generation reusable rocket turbopumps.

3. System Architecture and Design Considerations

3.1 Turbopump Architecture Selection: Rationale for Single-Shaft Configuration

This study investigates a single-shaft turbopump architecture aimed at supporting deep throttling operations in reusable liquid rocket engines. The selected reference configuration is inspired by the RL10 SSTP (Single Shaft Turbopump) architecture, which eliminates the geared train between the turbine and dual propellant pumps by using a common shaft. This configuration offers advantages in simplicity, weight reduction, and dynamic balancing.
Key advantages include the ability to throttle from 11,000 to 35,000 pounds of thrust, improved restart reliability, and reduced vibration due to the absence of gear meshing. Design trade-offs include the inability to individually optimize pump speeds for oxidizer and fuel, necessitating compromise in impeller sizing and boost pump integration.

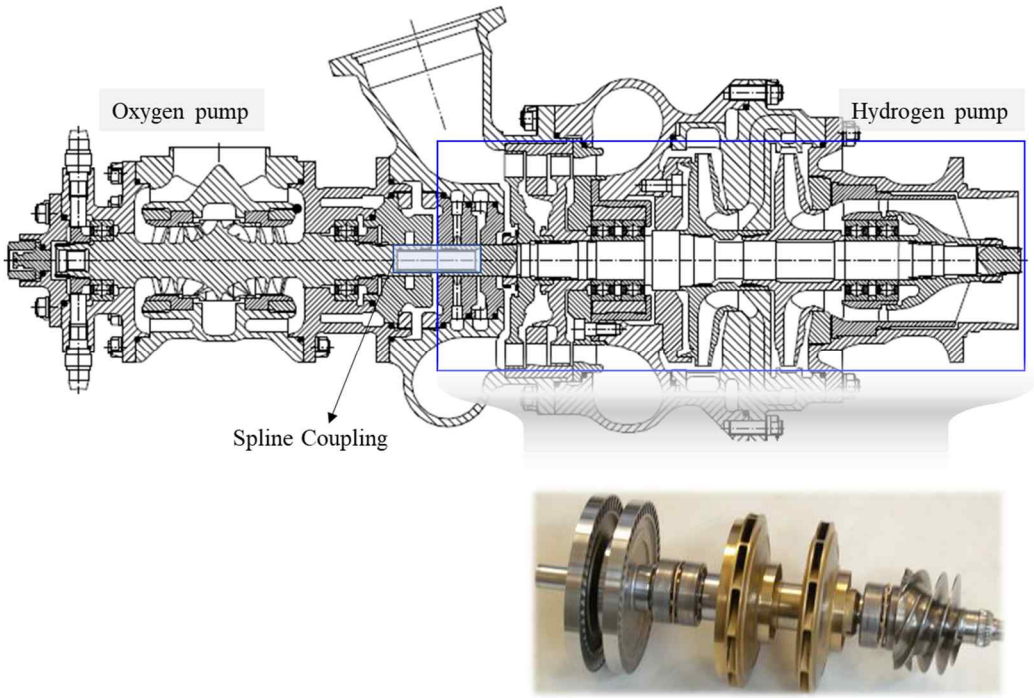

Figure 2: Layout of RL10 engine single shaft turbopump assembly [9]

Turbopump configurations can generally be categorized into dual-shaft and single-shaft architectures. Dual-shaft turbopumps, commonly used in staged combustion engines, allow independent optimization of fuel and oxidizer pump speeds, enabling high overall performance and operating flexibility. However, they typically require additional gearbox assemblies, increased structural complexity, and more challenging rotor dynamic balancing due to multiple rotating shafts.
In contrast, single-shaft turbopumps—as illustrated in Figure 3—combine the turbine and both propellant pumps on a common shaft. This configuration reduces mechanical complexity, eliminates the need for speed-matching gear trains, and facilitates better mass balance and structural simplicity. Importantly, the single-shaft design offers enhanced mechanical robustness and dynamic symmetry, which are advantageous under variable-thrust or throttling environments where system disturbances and load transients are more frequent.
In this study, the single-shaft turbopump architecture was selected as the baseline configuration to explore its dynamic behavior under deep throttling conditions. The simplified rotor layout minimizes phase lag and torque ripple between stages, while allowing for an integrated sealing strategy that ensures strict isolation between the two cryogenic propellants—liquid oxygen (LOX) and liquid methane (LCH)—to prevent cross-contamination across the shared shaft

DOI: 10.13009/EUCASS2025-415

structure. These features make the single-shaft system particularly suitable for deep throttling operations in reusable engine cycles, where repeatable ignition and stable low-thrust performance are critical.

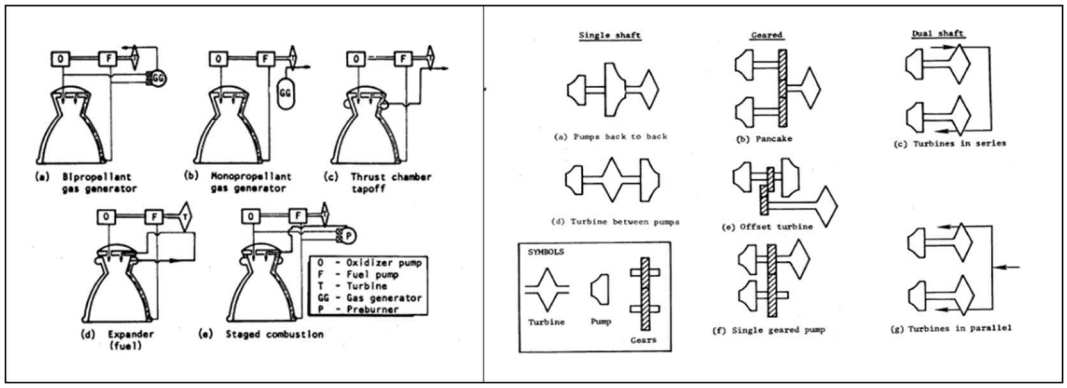

Figure 3: Overview of turbine arrangements based on engine cycles and turbopump arrangements

3.2 Rotor – Bearing System Overview

Figure 4 provides a schematic representation of the rotordynamic model architecture for a reusable methane turbopump, highlighting the relative positions of major components such as the liquid methane pump, oxidizer pump, turbine, and their associated bearings and seals. The turbine is centrally located between the LOX and LCH_4 pumps to ensure mechanical symmetry and reduce cross-coupled thermal effects. Bearing positions are carefully arranged to manage the distribution of axial and radial loads while minimizing shaft deflection and maintaining critical speed margins. The placement of floating ring seals near each pump stage is also shown, reflecting their role in isolating cryogenic fluids and controlling leakage under high-speed operation. This integrated layout serves as the geometric basis for subsequent rotordynamic and thermal–mechanical simulations described in Section 4.

In this single-shaft configuration, the LOX pump incorporates a double-suction impeller with a boost inducer to mitigate cavitation risk, whereas the methane pump employs an axial-centrifugal impeller sequence optimized for low inlet pressure conditions. To control the rotordynamic response, elastic damping elements are integrated into the bearing supports. A typical bearing arrangement includes duplex angular contact ball bearings combined with corrugated plate-type supports that absorb transient loads and suppress high-frequency oscillations. Design considerations also include shaft alignment and thermal expansion tolerances to ensure consistent dynamic performance throughout the full operating range.

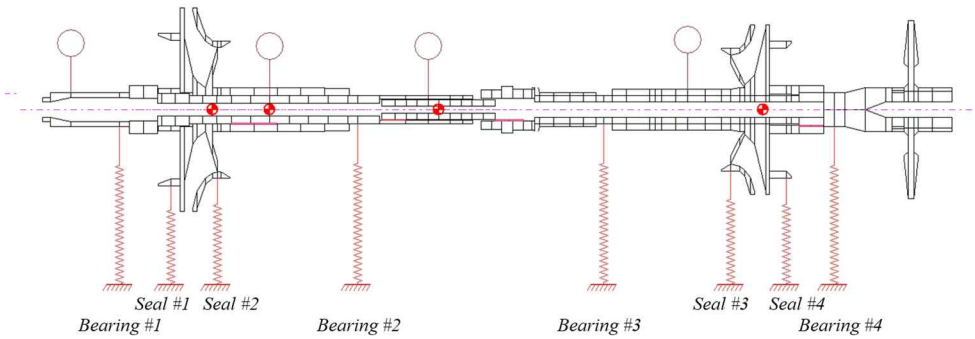

Figure 4: An example of a rotordynamic model with bearings and seals location for a reusable methane turbopump

4. Rotordynamic Modeling and Parametric Study

4.1 Dynamic Model Formulation

The dynamic response of the rotor-bearing-seal system is modeled using an extended version of Childs' linearized formulation. The full equation of motion includes mass (M), stiffness (K), and damping (C) matrices, with cross-coupled terms representing fluid-induced destabilizing forces. The governing equation is:

DOI: 10.13009/EUCASS2025-415

$$M \cdot \ddot{q}(t) + C \cdot \dot{q}(t) + K \cdot q(t) = F(t) \quad (3)$$

The stiffness and damping matrices include thermal correction factors and nonlinear stiffness terms derived from contact mechanics under preload. These allow simulation of rotor behavior across a wide throttling envelope.
Simulation scenarios include stepwise changes in shaft speed, inlet temperature, and axial load. Boundary conditions are selected to replicate operational phases such as ignition, deep throttling, and shutdown. Key parameters such as fluid viscosity, bearing clearance, and support stiffness are varied within realistic ranges to assess sensitivity.
Rotordynamics analysis software, *Dyrobes* are used to integrate time-domain responses and extract critical speed crossings, amplitude growth near resonance, and damping ratio variations. A modal reduction technique is applied to enhance computational efficiency while preserving dominant dynamic modes.
Figure 5 shows flowchart outlines the conceptual design process for a turbopump's rotordynamic model. It begins with defining initial requirements and then proceeds with a 1D sizing and performance mapping of the pump. The process then branches based on whether performance requirements are met, leading to either revisions or continuation with shaft diameter and maximum speed selection. Dynamic characteristics of bearings and seals are calculated, feeding into the rotordynamic design phase. Finally, the process concludes with completion of the conceptual rotordynamic model design if the critical speed margin is satisfied.

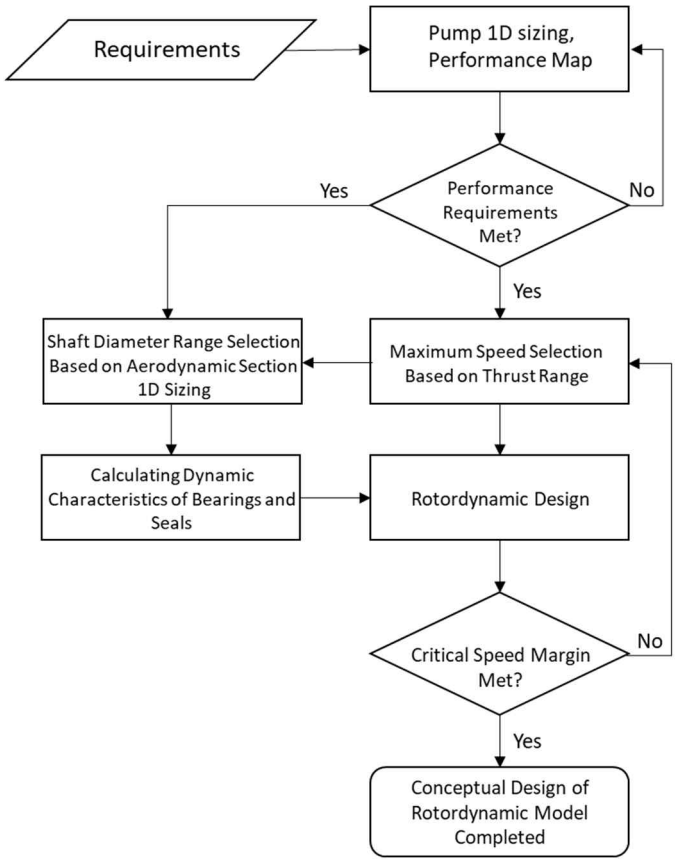

Figure 5: Turbopump rotordynamic conceptual design flowchart

4.2 Critical Speed Analysis

Critical speeds are identified through FFT analysis and eigenvalue tracking. The system exhibits multiple critical frequencies, especially in the hydrogen pump rotor segment. Damping effects are evaluated by varying support stiffness and bearing preload, showing that sufficient damping can shift or suppress instability zones.
A critical speed map is constructed as a function of shaft speed and thrust level, highlighting safe operating regions. The map illustrates how dynamic stability is compromised when combined effects of thermal growth and reduced damping converge near specific operating points. Design recommendations are drawn from this analysis to guide operational envelope setting.

DOI: 10.13009/EUCASS2025-415

Figure 6 shows the preliminary critical speed analysis results for a single-shaft turbopump rotating assembly. The plot illustrates the variation in critical speed as a function of shaft rotational speed and system configuration, emphasizing the proximity of operational speed ranges to the first and second critical modes. The results indicate that, without sufficient damping or appropriate design modifications, resonance phenomena may arise within the expected throttling range. In particular, the turbopump segment exhibits a pronounced peak in response amplitude near the first critical speed, underscoring the need for precise tuning of bearing stiffness and preload conditions.
Figure 7 describes how minor modifications to shaft geometry can effectively increase the margin between critical speeds and operating ranges. However, the achieved margin still falls short of the standard design criterion, which typically requires exceeding an 18% safety margin under baseline rotor design conditions.

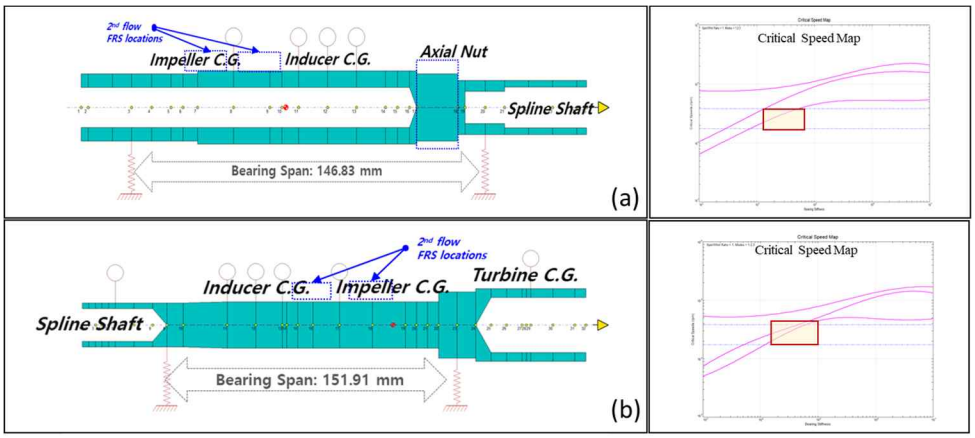

Figure 6: Preliminary Critical Speed Analysis Results for a Single-Shaft Turbopump Rotating Assembly

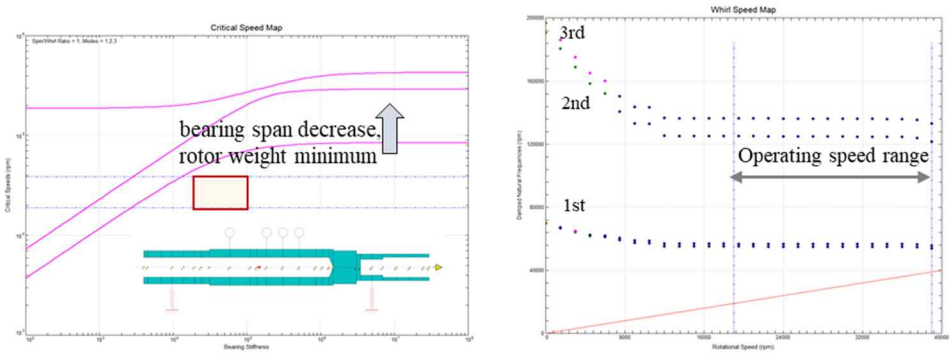

Figure 7: Securing Critical Speed Margin through Shaft Geometry Modification

4.3 Thermal Preload Model and Contact Force Formulation

Thermal deformation plays a critical role in altering bearing contact conditions and preload. As the shaft and surrounding structures heat up under cryogenic-to-ambient transitions, both axial and radial displacements occur. These changes affect the contact angle, internal clearance, and ultimately the stiffness matrix of the bearing.
To account for these effects, the design integrates temperature-dependent preload calculations into the bearing model. The inner race expansion, centrifugal growth of the balls, and viscosity-dependent damping coefficients are modeled to reflect real operating conditions. This thermal-mechanical coupling is crucial for predicting the correct dynamic response under transient throttling cycles.

DOI: 10.13009/EUCASS2025-415

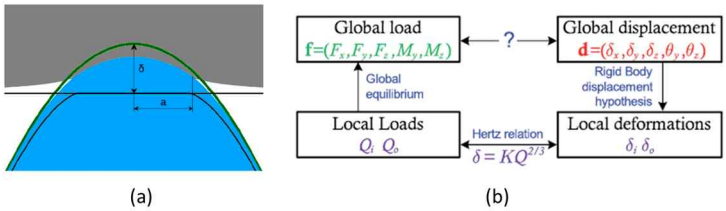

Figure 8: (a) Deflection due to contact between an elastic sphere, $\boldsymbol{\delta}$ and (b) an elastic plane
Radius of the circular contact area, $\boldsymbol{\alpha}$

In this section, the analytical formulation used to capture thermal deformation-induced preload changes is described in detail. As the bearing components are subjected to temperature gradients during throttling operations, differential expansion occurs among the inner race, outer race, and rolling elements. These dimensional changes directly influence contact angle α, internal clearance δ, and ultimately, the contact force and stiffness matrix.
The preload variation $F_p(T)$ as a function of temperature is derived from the effective radial interference between inner and outer rings, including centrifugal effects:

$$\delta_{eff}(T) = \delta_0 - \Delta r_{therm\,al}(T) + \Delta r_{centrifugal}\quad(\omega) \tag{4}$$

where:

- δ_0 is initial clearance at assembly,
- $\Delta r_{therm\,al}(T) = \alpha_{m\,aterial}\cdot\Delta T + D$ are the radial thermal expansion,
- $\Delta r_{centrifugal}\quad(\omega) = \frac{\rho_{ball}\cdot\omega^2\cdot D^2}{2E}$ are centrifugal-induced deformation,
- D is pitch diameter of bearing
- $\alpha_{m\,aterial}$ is thermal expansion coefficient of steel or ceramic material (bearing materials)
- ω is angular velocity.

The resulting preload force is approximated using Hertzian contact theory as:

$$F_p = k_H \cdot \delta_{eff}^{3/2} \tag{5}$$

with k_H being the Hertzian contact stiffness coefficient, determined by the bearing geometry and material properties. The contact angle α is updated at each iteration using the geometric relationship for ball bearings:

$$\tan(\alpha) = F_a/(F_r + F_p) \tag{6}$$

This angle influences the directional components of stiffness:

$$\left.\begin{aligned} K_x &= N\cdot k_c\cdot cos^{\,2}(a)\\ K_y &= N\cdot k_c\cdot sin^{\,2}(a)\end{aligned}\right\} \rightarrow K_{bearing} = \begin{bmatrix} K_x & 0\\ 0 & K_y\end{bmatrix} \tag{7}$$

Where:

- N is number of balls,
- k_c is the single contact point stiffness,
- F_a, F_r are axial and radial loads applied to the bearing.

This coupling allows the bearing stiffness matrix to evolve dynamically with operating temperature and shaft speed:

$$K_{bearing}\quad(T,\omega) = \begin{bmatrix} K_x(T,\omega) & 0\\ 0 & K_y(T,\omega)\end{bmatrix} \tag{8}$$

The damping matrix $C_{bearing}$ is also updated based on temperature-dependent viscosity $\mu(T)$ and bearing geometry:

DOI: 10.13009/EUCASS2025-415

$$C_{eq}(T) = C_0 \cdot \left(\frac{\mu(T)}{\mu_{ref}}\right)^{\beta} \tag{9}$$

This thermally-awre model is implemented in MATLAB using temperature-coupled iterations, where the effective preload is recalculated at each timestep and updates the system matrices *K, C*, contact angle α.

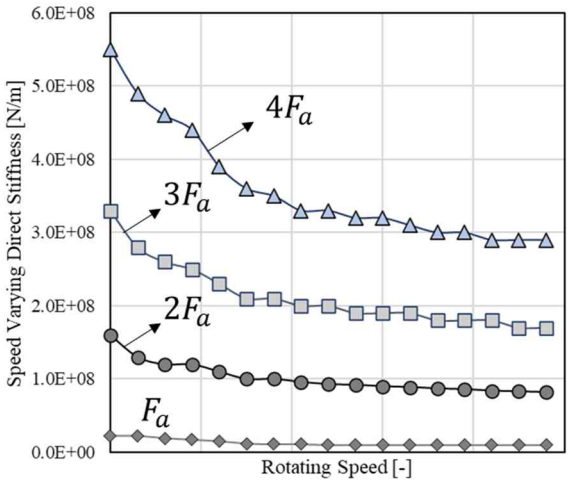

Figure 9: Influence of speed on direct stiffness of bearings under various axial loads

4.4 Floating Ring Seal Dynamics and Rotor Interaction

Figure 10 describes the differential pressure branching caused by secondary flow in the floating ring seals (FRS) located at the front and rear of the impeller. During the initial operation of the turbopump, the fluid forces acting on the floating ring are small, allowing it to float freely within the working medium due to the relative rotational motion between the impeller and the pump stationary end. However, at rated rotational speed, the fluid pressure causes the floating ring to find and adhere to an appropriate eccentric position on the support ring, thereby regulating the leakage flow.

Specifically, in high-speed and high-pressure environments, dynamic forces are generated due to the relative behavior of the seal resulting from slight whirling motions of the rotating components. These forces act as reactions within the seal and gap, potentially influencing the rotating components, making it necessary to predict the seal's dynamic coefficients during the rotor design stage

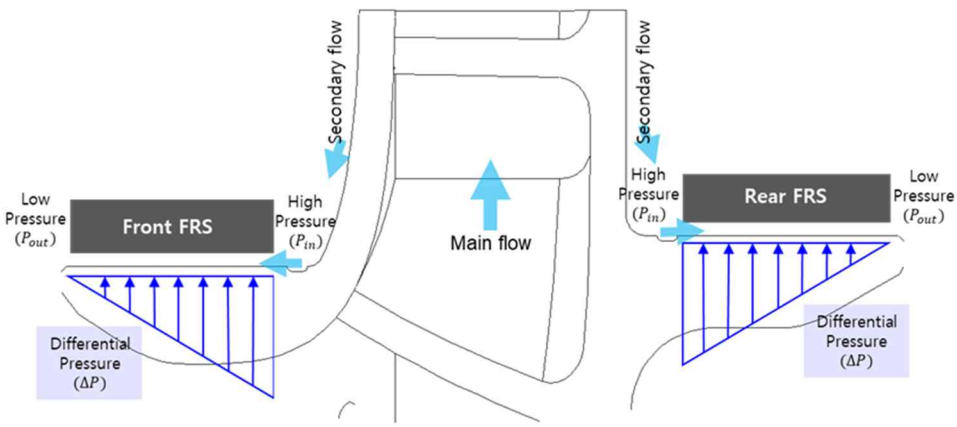

Figure 10: Pressure distribution due to secondary flows in front and rear floating ring seals of an Impeller

Dynamic characteristics primarily refer to stiffness and damping coefficients. Because these characteristics change depending on operating conditions due to the physical changes in fluid behavior with rotational speed, a dynamic

DOI: 10.13009/EUCASS2025-415

characteristic analysis is essential. Figure 11 presents the results of a dynamic characteristic analysis performed with a seal length of 7.5 and 9.5 mm under differential pressures of 5, 6, and 10 MPa. While leakage flow rate and pressure from the impeller will vary with rotational speed, in this stage of analysis, fluid properties were held constant, aside from rotational speed and seal geometry. The first result graph reveals that as rotational speed increases, the increase in axial Reynolds number due to the tangential direction causes a decrease in the force due to fluid dynamics, and consequently, a decreasing trend in direct stiffness. This is likely due to the use of a bulk-flow analysis model that assumes a fully developed shear flow in the gap between the seal and the impeller shroud outer surface. The model indicates that as speed increases, the circumferential velocity of the fluid approaches a limit tangential velocity. The cause of the negative direct stiffness lies in the direct stiffness formulation within the bulk-flow analysis model. It indicates that negative results occur when 1) sufficient differential pressure is not applied or 2) the seal length is insufficient. The analysis results in Figure 11 suggest that a negative stiffness arises because sufficient differential pressure was not applied. This can be observed by noting that, at the same rotational speed and the same differential pressure (5 MPa), the case with a shorter seal length of 7.5 mm exhibits a higher stiffness compared to the case with a seal length of 9.5 mm

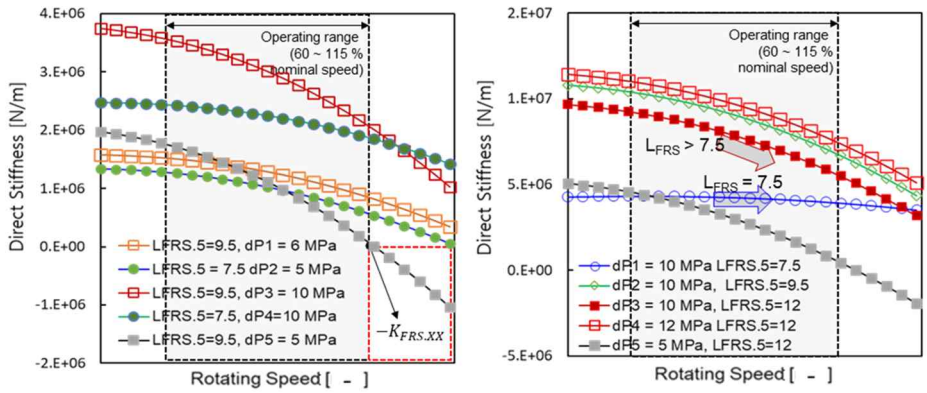

Figure 11: Stiffness characteristics of floating rings in a liquid oxygen environment as a function of geometry and differential pressure

5. Validation and Design Implications

5.1 Design Trade-offs for Throttling Operation

The trade-off between rotor simplicity and independent optimization is critically examined. While single-shaft architecture offers simplicity and reliability, it limits individual tuning of pump speeds. This necessitates the use of inducers, multi-stage pumps, or custom vane geometries to compensate.

Furthermore, balancing preload for cryogenic startup while avoiding over-constraining at ambient conditions requires fine-tuned thermal compensation mechanisms. The findings highlight the need for integrated thermo-mechanical design and validate the advantage of elastic damping structures in achieving robustness.

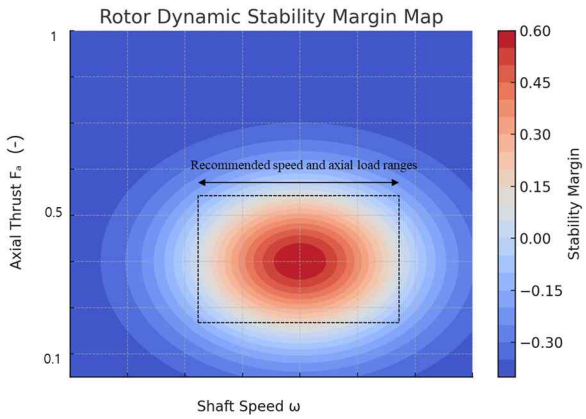

Figure 12: Rotordynamic stability margin map for a sing-shaft turbopump under large operating speed range

DOI: 10.13009/EUCASS2025-415

5.2 Startability and Restartability Considerations Under Cryogenic Damping Behavior

The preceding sections have demonstrated that thermally induced variations in lubricant viscosity significantly affect the damping characteristics of the bearing–support system. These variations, particularly under cryogenic conditions, are closely tied to operational challenges in turbopump start-up and restart processes.
The damping coefficient $C_{eq}(T)$, derived from temperature-dependent viscosity models of cryogenic propellants such as LOX and LCH4, increases exponentially as the temperature drops. This rise in damping is beneficial for stabilizing dynamic responses during throttling but also introduces considerable resistance during shaft spin-up. The associated frictional power loss, expressed as:

$$P_{bss} = C_{eq}(T) \cdot \dot{x}_{RMS}^2 \tag{10}$$

indicates that low-temperature start-up conditions impose higher torque demands to overcome viscous friction. For example, simulation results show that damping at 60 K is approximately three times higher than at 300 K, leading to a 300–400% increase in frictional loss for the same vibration velocity.
The observed distinction between startability and restartability across thermal regimes can be explained through the temperature-dependent behavior of the equivalent damping coefficient $C_{eq}(T)$. As the bearing environment transitions to cryogenic temperatures, the viscosity $\mu(T)$ of the lubricant increases exponentially, leading to a corresponding rise in damping:

$$C_{eq}(T) = C_0 \left(\frac{\mu(T)}{\mu_{ref}}\right)^{\beta} \tag{11}$$

This elevated damping increases the frictional resistance during spin-up, and the resulting power loss is approximated by equation 10. Where x_{rms} is the root-mean-square velocity of the rotor at low speeds. Consequently, the torque required to initiate rotation at cryogenic conditions becomes significantly higher:

$$T_{ref} = J \cdot \frac{d\omega}{dt} + C_{eq} \cdot \omega \tag{12}$$

This increased torqe demand negatively affects startability. In contrast, restartability issues arise not from frictional resistance, but from reduced damping at elevated temperatures. As $C_{eq}(T)$ decreases in ambient conditions, the rotor system becomes more susceptible to dynamic instabilities, particularly when the system is operating near critical speeds or under relaxed preload conditions. In such cases, the real part of system eigenvalues may approach zero or become positive, indicating potential for whirl-type instabilities (Table 1). Therefore, startability is primarily limited by frictional damping in cryogenic regimes, while restartability is more closely linked to insufficient damping-induced stability loss in warmer conditions. From a startability standpoint, this implies that excessive viscous drag at cryogenic temperatures may delay or prevent successful shaft acceleration unless sufficient starting torque is provided. Additionally, high contact angles under cold preload conditions may further stiffen the bearing system, amplifying the initial torque requirement.

Table 1: Temperature-dependent damping effects on startability and restartability

Temperature Regime	Damping Coefficient ($C_{eq}(T)$)	Friction Loss (P_{bss})	Startability	Restartability
Cryogenic (< 100K)	High	High	Challenging	Stable
Ambient (200 – 300K)	Low	Low	Easy	Potentially Unstable

In restart scenarios—typically performed after engine shutdown and thermal soaking—different considerations emerge. At elevated restart temperatures (150–300 K), the damping may be insufficient to suppress rotor instabilities, especially

DOI: 10.13009/EUCASS2025-415

if preload has relaxed due to thermal expansion. This asymmetry in damping performance across operational cycles affects restart reliability and warrants tailored thermal management.
To mitigate these challenges, design strategies such as adaptive preload mechanisms, elastic bearing supports, or controlled thermal soak-up prior to restart may be employed. Furthermore, a low-speed transient simulation including temperature-dependent friction torque can help define reliable operating envelopes for successful engine ignition and re-ignition.
This analysis highlights the need to consider both ends of the temperature-damping-performance spectrum when developing reusable turbopumps for deep-throttling engines. Future work will extend the present model by incorporating startup motor characteristics, shaft inertia, and cryogenic torque maps to provide full predictive capability for mission-critical start–stop sequences.

6. Conclusion

The rotordynamic analysis framework developed in this study has enabled a sequential evaluation of system behavior under deep throttling conditions, incorporating thermal–mechanical coupling, preload variations, and dynamic component characteristics. Key findings derived from Sections 3 to 5 are summarized as follows:
1. While the single-shaft turbopump architecture, originally designed for gas-generator cycle engines, demonstrated sufficient dynamic stability at nominal conditions, its application under deep throttling revealed a significantly reduced margin with respect to critical speed crossings. The broadened operational envelope led to potential proximity to the first or second critical speeds, raising concerns about dynamic robustness.
2. The incorporation of thermal deformation-induced preload into the dynamic model further demonstrated that preload variations caused by cryogenic-to-ambient thermal transitions can critically influence bearing stiffness and damping. This variation reduces the predictability of stability margins and may lead to instability if not properly compensated during design.
3. Parametric studies involving updated bearing and seal dynamic coefficients, derived from thermal and speed-sensitive models, showed that the inclusion of realistic stiffness and damping behavior tends to significantly reduce the available critical speed margin, necessitating more conservative margin definitions and design adjustments. Particularly, cross-coupled stiffness and damping effects from seals further exacerbate potential whirl instabilities.
4. These findings emphasize that in deep throttling scenarios where the turbopump must operate over an extended speed range, the dynamic response of the rotor assembly must be thoroughly assessed and integrated into the design process. Neglecting this consideration may result in overlooked instability zones and compromised reliability, especially in engines requiring multiple ignitions or throttling cycles.
In light of these observations, the use of coupled thermal–rotordynamic analysis, incorporating accurate preload and component-specific behavior, is essential to ensure robust design. The proposed modeling approach provides a practical methodology for identifying operating limitations and guiding stability-conscious hardware development for future deep throttling reusable engines. This integrated approach contributes to enhancing the durability and operational reliability of reusable liquid rocket engines by maintaining dynamic stability throughout the full throttling envelope, thereby supporting reliable multi-cycle operation.

References

[1] Theunis, H. J. du T., Valentyn, B., and Vasileios, P., “European Staged Combustion Rocket Engine Technology Roadmap,” *9th Space Propulsion Conference*, Paper No. 424, 2024.

[2] D. W. Childs, and J. B. BATES Ⅲ, “Residual-Flexibility Corrections for Transient Modal Rotordynamic Models,” *Journal of Mechanical Design*, Vol.100, 1978, pp.251-256

[3] Zhang, Y., Wang, J., and Li, H., “Effect of Interference Fit, Rotational Speed, and Radial Load on Bearing Stiffness with Inner Ring Elastic Deformation,” Mech. Syst. Signal Process., Vol. 185, 2023, pp. 109082.

[4] Gunduz, A., and Singh, R., “Stiffness Matrix Formulation for Double-Row Angular Contact Ball Bearings,” *J. Mech. Des.*, Vol. 131, No. 4, 2009, pp. 042602.

[5] Suresh M. S., “Development of Turbopump Systems for Cryogenic and Semicryogenic Propulsion Systems of ISRO,” *Transactions of the Indian National Academy of Engineering*, Vol. 6, 2021, pp.229-241

[6] Lei, Y., Zhang, H., and Li, C., “An Integrated Stiffness Model of Ball Bearings Considering Elastic, Centrifugal and Thermal Effects,” *Int. J. Mech. Sci.*, Vol. 215, 2022, pp. 106986.

[7] Deng, S., Shen, J., Yang, C., Qian, D., and Hua, L., “Influence of Various Balls and Groove Curvature Radii on Dynamic Stiffness of Ball Bearings Based on Nonlinear Dynamic Model,” *Appl. Math. Model.*, Vol. 127, 2024, pp. 259–280.

DOI: 10.13009/EUCASS2025-415

[8] Xu, C., Zhang, T., and Yang, Y., “Mathematical Modeling and Analysis of Duplex Angular Contact Bearings under Misalignment,” *Tribol. Int.*, Vol. 170, 2022, pp. 107485.
[9] Rachuk V. S. and Dmitrenko A. I., “Single Shaft Turbopump Expands Capabilities of Upper Stage Liquid Propulsion”, *44th AIAA/ASME/SAE/ASEE Joint Propulsion Conference & Exhibit*, 21-23 July 2008